THE ASTROPHYSICAL JOURNAL, 240:161–168, 1980 August 15

THE ULTRAVIOLET SPECTRUM AND FLUX OF HD 152667 (=X-RAY SOURCE 1653−40?)

J. B. HUTCHINGS[1]
Dominion Astrophysical Observatory, Herzberg Institute of Astrophysics
AND
A. K. DUPREE[1]
Harvard-Smithsonian Center for Astrophysics
Received 1979 December 17; accepted 1980 February 28

ABSTRACT

IUE data are presented on the massive binary system HD 152667 (spectral type BO I), covering many phases of the 8 day orbit. Low-dispersion data are used to drive $T_{\rm eff}$, E_{B-V}, and the UV light curve. The secondary object is much fainter than the primary at all wavelengths. The stellar wind shows complex multiple components and is unique in our experience. A weak, variable distortion of the wind may be present near superior conjunction of the primary. Weak lines show the primary orbital motion, with minor distortions. The interstellar absorption spectrum shows high temperature species most probably arising in the H II region produced by the star. No clear evidence is found regarding the nature of the secondary object. Discrepancies in published ephemerides of the system are clarified.

Subject headings: stars: early-type — stars: individual — stars: winds — ultraviolet: spectra — X-rays: binaries

I. INTRODUCTION

The massive interacting binary HD 152667 was suggested as the optical counterpart to a weak X-ray source detected by the *Copernicus* satellite (Polidan *et al.* 1978) on the basis of its having an unseen companion of $\sim 7\ M_\odot$. The primary star is a BO supergiant near the bright open cluster NGC 6231, and optical studies have been made by Walker (1971), Hill, Crawford, and Barnes (1974), Hutchings (1979*a*), Massey *et al.* (1979), and Wolff and Beichmann (1979). The system has a period of ~8 days, and there is no direct evidence of the nature of the secondary star. The system has an ellipsoidal light curve whose amplitude suggests that shallow eclipses occur as well as the changes caused by gravitational distortion of the primary. The primary star shows a strong stellar wind which seems to be variable over a time scale of years, or possibly months. The stellar wind from the primary is seen to be phase dependent. There is no evidence of He II λ4686 emission, the usual signature of an X-ray binary with a compact companion.

A near coincidence between X-ray turn-on in the field and a unique C III λ1176 line-emission flare, observed with the *Copernicus* satellite (Polidan *et al.* 1979) strengthened the case for the system being an X-ray binary. However, it was shown by White and Pravdo (1979) that there is a 38 s period X-ray pulsar some 30′ away from HD 152667, which almost certainly would have been in the *Copernicus* X-ray beam. Subsequent pointings with the *Einstein* observatory have not confirmed the detection of X-rays from HD 152667 to limits well below the *Copernicus* limits (Holt 1979) at phases when the companion was not occulted by the primary. We also note that Polidan *et al.* (1979, Fig. 3) detected X-rays through $\phi_x = 0$ which is curious in view of the evidence for optical eclipses in the system. Thus it is clear that if it is a source at all, the binary is normally a very weak one, with a luminosity probably well below 10^{33} ergs s^{-1}. In view of the strong stellar wind from the primary, this means that if X-rays are generated near a compact companion, they must be heavily blanketed by supercritical accretion.

The *IUE* data were obtained with the purpose of studying (a) the mass flow as a function of orbital phase, as seen in the UV resonance lines; (b) the continuum for color and intensity changes which may contain clues as to the nature of the secondary; and (c) to look for signs of ionization holes in the wind produced by X-rays. These latter effects were found in HD 77581 (Vela X−1) and HDE 226868 (Cyg X−1) by Dupree *et al.* (1978, 1980).

Table 1 summarizes the *IUE* spectroscopic observations. Figure 1 shows a mean low-dispersion spectrum in the short λ region. The spectrum is typical of a moderately reddened B0 supergiant, showing strong P Cygni profiles of Si IV and C IV and absorptions of subordinate lines appropriate to the photospheric temperature.

II. TIMING AND PHASING

It is vitally important to establish an ephemeris for the system in order to relate optical (and X-ray)

[1] Guest Observers, *International Ultraviolet Explorer* satellite.

TABLE 1

SUMMARY OF OBSERVATIONS

Image	Aperture	Exposure Time	Dispersion	Date (UT.) 1978	Date (J.D) (2440 000 +)	Phase[a]
SWP		Min:Sec				
SWP 1959	S	18:0	H	July 10 17:8:0	3700.22	0.01
SWP 1993	S	22:0	H	July 13 16:42:0	3703.20	0.39
SWP 2010	S	25:0	H	July 14 18:07:0	3704.26	0.52
SWP 2101	S	25:0	H	July 25 14:4:52	3715.10	0.90
SWP 2102	S	0:12	L	July 25 15:04:0	3715.13	0.91
	L	0:12	L	July 25 15:09:0		
SWP 2155	S	0:18	L	July 30 18:29:0	3720.27	0.56
	L	0:18	L	July 30 18:32:52		
SWP 2156	S	35:0	H	July 30 19:28:42	3720.31	0.57
SWP 2366	S	30:00	H	Aug. 22 16:36:07	3743.20	0.48
SWP 2367	S	0:10	L	Aug. 22 17:06:0	3743.22	0.48
	L	0:5	L	Aug. 22 17:10:0		
SWP 2916	S	30:00	H	Oct. 11 9:38:34	3792.91	0.82
SWP 2917	S	0:30	L	Oct. 11 10:11:0	3792.92	0.82
	L	0:20	L	Oct. 11 10:15:0	3792.92	
SWP 2948[b]	S	30:00	H	Oct. 13 2:27:31	3794.62	0.03
SWP 2949	S	0:30	L	Oct. 13 2:59:0	3794.62	0.03
SWP 2981	S	0:30	L	Oct. 15 1:04:0	3796.54	0.28
	L	0:20	L	Oct. 15 1:11:0		
SWP 2982	S	30:00	H	Oct. 15 2:01	3796.58	0.28
SWP 3005	S	30:00	H	Oct. 17 8:38:16	3798.84	0.57
SWP 3006	S	0:30	L	Oct. 17 9:07:0	3798.88	0.58
	L	0:20	L	Oct. 17 9:11:30		
LWR						
LWR 1828	L	00:11	H	July 14 19:14:0	3704.30	0.53
LWR 1924	S	15:00	H	July 30 19:13:28	3720.31	0.57
LWR 2150	S	15:00	H	Aug. 22 17:38:57	3743.24	0.49
LWR 2573	S	25:00	H	Oct. 11 11:08:06	3792.97	0.83
LWR 2589	S	20:00	H	Oct. 13 3:49:55	3794.66	0.04
LWR 2605	S	20:00	H	Oct. 15 1:48:35	3796.58	0.28
LWR 2629	S	20:00	H	Oct. 17 9:57:27	3798.92	0.58

All dates refer to mid-exposure time.

[a] $\phi_x = 0$ at JD 2440812.01+7.84825E.

[b] grossly underexposed image, not useable.

variability in terms of eclipses and other phase-dependent quantities. Unfortunately the literature on the system contains some confusing errors. Some of these were discussed by Hutchings (1979*a*), who gave a new orbit and time of secondary superior conjunction ($\phi_x = 0$). A later discussion of the orbit by Wolff and Beichmann (1979) unconventionally gives phases from minimum velocity, while quoting T for a noncircular orbit. We have now combined all of the Wolff and Beichmann Si IV data with the Si IV and N III data of Hutchings. The computed orbital parameters for $e = 0$ yielded JD 2,440,813.97 $\pm$ 0.05 for time of *maximum* velocity for all data and for both subsets of data, which corresponds to $\phi_x = 0$ at JD 2,440,812.01. This is compatible with all published ephemerides, and is adopted in this paper.

Note that the phases used here are from the predicted time of X-ray mid-eclipse (superior conjunction of the secondary star) and should be correct to better than 0.01 phase.

III. LOW-DISPERSION DATA

All low-dispersion spectra were obtained with both apertures. The main purposes of these observations

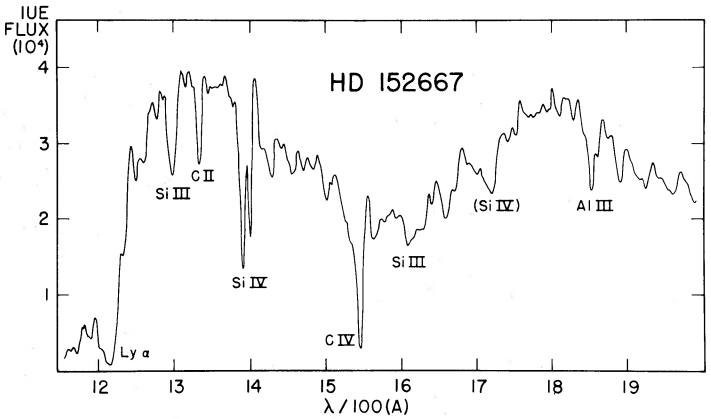

FIG. 1.—Mean of large and small aperture spectra of HD 152667 at low dispersion. *IUE* fluxes given for 20 s exposure in large aperture. Principal line features are identified, those in brackets being principal contributors to a blend.

were (1) to look for changes with phase in the energy distribution and intensity and (2) to derive estimates of $T_{\rm eff}$ and interstellar extinction, using the *IUE* low-dispersion calibration.

A continuum was estimated on all low-dispersion data measured at six wavelengths. Each represents an integration of roughly 100 Å and ignores line features. In order to enable proper allowance to be made for line blends, in making the continuum level estimates, high-dispersion data were plotted with spectral resolution degraded by varying amounts.

The large aperture data were used for photometry. The intensity in each wavelength bin showed phase-related changes which were the same in each bin to within the accuracy of the measures and the reproducibility of the *IUE* instrument ($2\sigma = 10\%$). These fluxes were combined to form the mean light curve shown in Figure 2.

The UV light curve has a larger amplitude than the visible light curve before 1972, observed by Cousins and Lagerwey (1969), and in particular the $\phi = 0.5$ minimum is considerably deeper. This suggests that the surface brightness in the UV of the secondary is fainter than the primary. Since the difference between primary and secondary eclipse depths is less in the visible, we can conclude that the secondary is cooler than the primary.

Computed light curves for $M_1/M_2 = q = 3.5$ and $T_{\rm eff} = 25{,}000$ K for the primary yield amplitudes which are approximately twice as large at $\lambda 1500$ as at $\lambda 5500$. This is in rough agreement with the data. The eclipse depth ratio then indicates that $T_{\rm eff}$ of the secondary light sources is $\sim 19{,}000$ K, assuming a normal thermal model for the secondary. As for the B, V light curves, some secondary light is required to model the observed eclipse depths. See Walker (1971) and Hutchings (1979*a*) for discussion of the light curves.

The fine error sensor (FES) of *IUE* can be used as a $\sim V$ band photometer. The shape for the V light curve from the FES counts is different from that published by Cousins and Lagerwey and does not fit the simple model as well. It is clearly important to do a proper photometric investigation to see if this change is real. The $\lambda 1500$ light curve has the same shape as the FES visual light curve. Both of these curves can be fitted better (at $\sim 1\sigma$ level) with a small eccentricity (0.03) in the orbit and $\omega = 90°$ than with a circular orbit model. This is compatible with the spectroscopic orbit, but not very significant.

The mean spectral distribution was derived from all low-dispersion data and converted to fluxes using the

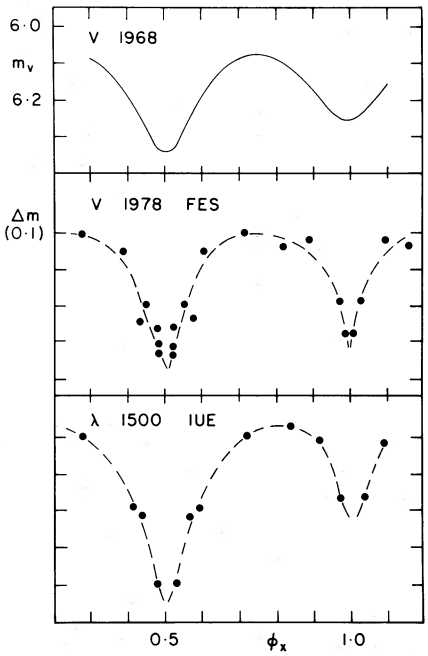

FIG. 2.—Light curves of HD 152667. *Upper.*—curve is V data from Cousins and Lagerwey (1969). *Center.*—1978 data from *IUE* fine error sensor whose sensitivity is close to V band. Note apparent change from upper V curve. *Lower.*—fluxes in $\lambda\lambda$ 1200–1900 region from *IUE* low-dispersion data. Note larger amplitude of UV light curve. Dashed lines are spline fits to data. All *IUE* points have been reflected about phases 0.0 and 0.5.

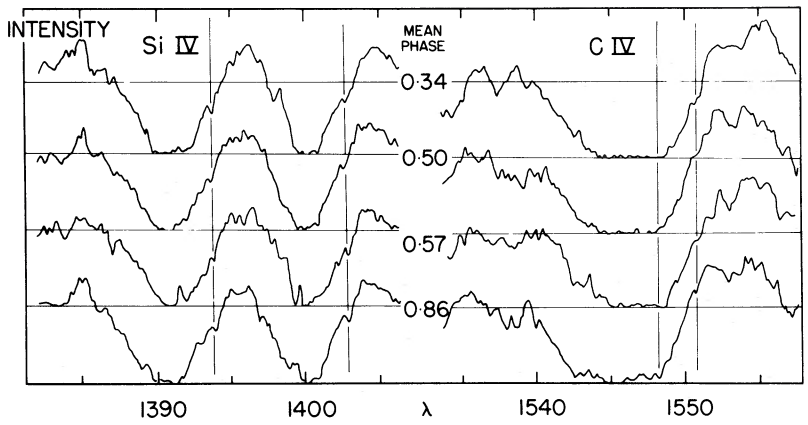

FIG. 3.—SWP high-dispersion Si IV and C IV resonance line profiles. Each tracing is the mean of two spectra, smoothed over 0.15 Å, separated by <0.1 phase. Vertical scale divisions are continuum height.

IUE calibration of Bohlin and Snijders (1978). These were then fitted to model atmospheres of Kurucz (1979) for $\log g \sim 3$, with several trial values of E_{B-V}, assuming a mean interstellar extinction. The best values lay in the range $E_{B-V} = 0.4$ to 0.5 and $T_{\rm eff} = 20$–24×10^3 K. A self-consistency check on the luminosity deduced from the stellar radius and temperature indicates a best value of $T_{\rm eff}$ of 23,800 ± 500 K and $E_{B-V} = 0.50 \pm 0.02$. This temperature is about right for a B0.5 I spectrum (Flower 1977). Absolute fluxes for a distance of 2 kpc yield consistent values of $T_{\rm eff}$ and E_{B-V} and are consistent with the TD-1 UV fluxes of Thompson *et al.* (1978) for this star.

The integrated energy for the fitted de-reddened spectrum is extrapolated to be $\sim 2 \times 10^{-6}$ ergs cm^{-2} s^{-1}. If the source is at 2 kpc, the luminosity is 7×10^{38} ergs s^{-1}. The optical luminosity estimate of $M_{\rm BOL} \sim -9.7$ (Hutchings and von Rudloff 1980) corresponds to 2×10^{39} ergs s^{-1}. These estimates are probably within the uncertainties in both quantities, and simply serve to confirm the high luminosity and the reddening value.

IV. THE N V, Si IV, C IV RESONANCE LINES

Figure 3 shows binned mean profiles of some of these lines ordered in orbital phase, smoothed over ~0.2 Å and normalized to the same continuum level. There are no very marked changes with phase, and the two observations at the same (0.57) phase in separate cycles suggest that nonperiodic changes are just as significant. Table 2 presents radial velocity measurements.

There are some points to note. First, some profiles at phase 0.57 have narrower cores, with a shoulder on the shortward wing. This is the same effect as is seen in the X-ray binary HD 77581 by Dupree *et al.* (1980), which they attribute to an ionization bubble surrounding the X-ray source. In HD 152667, it is noteworthy that the effect is not seen as strongly in the $\phi = 0.48$ or $\phi = 0.52$ spectra. It seems that in this spectrum the region of (occasionally) reduced line absorption trails the secondary and may, therefore, not be attributable to the same cause. We should therefore consider whether such an effect may arise by shadowing of the wind by a main-sequence secondary or by a dense gas stream from the primary. These questions may be clarified by studying other binary systems with winds, such as HD 47129, HD 57060, HD 1337. Note, too, that Fahlman and Walker (1979) find evidence for an off-axis gas stream in the X-ray binary system HD 153919, which is most evident at phase 0.63. Other measures on the lines (equivalent width, FWHM) show that changes are certainly seen at the 20% level, but it is not clear that they are phase related within the phase resolution (≥ 0.2) of our data. Since the continuum is known to vary over a range of ~25%, systematic apparent emission line changes of this amplitude may be seen without a real change in the emission intensity.

The signal at the N V λλ1237–1242 lines is weak in this reddened spectrum, but the lines do not appear to have very marked P Cygni characteristics. They are not detected in the $\phi_x = 0.01$ image, nor is the Si II λ1248 blend. On the low-dispersion image at $\phi_x = 0.03$, this

TABLE 2

HD 152667 RADIAL VELOCITIES

Line	Mean Radial Velocity (km s^{-1})
Optical	−20[1] to −45[1]
IUE Fe III weak	−425
C II	−575
Si III	−70[1], −575
Mg II resonance	−50,[1] −450[1]
Al III resonance	−430,[1] −650
N V resonance	−500:
Si IV resonance	−590, −1430 edge
C IV resonance	−730, −1440 edge

[1] Orbital motion evident.

Si II line feature is weaker than at other phases. In addition, the sharp absorption of Si II at $\lambda 1527$ is absent only on this image. The N V disappearance, if real, is similar to that seen in β Lyr (Hack *et al.* 1977) where the implication was that the line arises in the region between the stars and is eclipsed only by the larger stellar component. The simultaneous disappearance of Si II is peculiar and, in view of the uniqueness of the $\phi = 0$ image and its somewhat weaker exposure, should be confirmed by re-observation.

The velocity shifts of the resonance lines show no significant changes with phase, so that the lines are formed in the outer parts of the wind lying outside both component stars and are unaffected by their binary motion which from the photospheric lines indicate $k \sim 100$ km s^{-1}. The shifts are normal for the primary star mass and luminosity (Hutchings and von Rudloff 1980). Hutchings and von Rudloff (1980) derive a mass-loss rate of $9 \times 10^{-6} M_{\odot}$ yr^{-1} from the resonance line profiles of HD 152667. They note, however, that such determinations at present are very uncertain.

In the mean profiles of Si IV it is possible to fit the best position for the weak metallic (mostly Fe III) lines by sliding the pattern as a group. This position is indicated in Figure 4 and corresponds to a velocity of -425 km s^{-1}. A similarly shifted set of weak lines is seen in P Cyg and ζ^1 Sco (Hutchings 1979*b*), but the velocities in these stars are lower. The diagram also shows the spectrum of the B0 supergiant HD 105056 for comparison. In this, the Fe III lines fit best at -130 km s^{-1}. The wind in HD 152667 thus involves weak lines at much higher velocities than normal. The Si IV profiles themselves are less saturated in HD 152667 than HD 105056 but the opposite is true of the C IV lines. The star 26 Cep (HD 213087, B0.5 Ib) shows a complex Si IV absorption which is less saturated. Hutchings and von Rudloff (1980) show that Si IV saturation varies most rapidly with spectral type at about B0.5. Thus, the detailed ionization balance in these stellar envelopes varies between similar stars and with time.

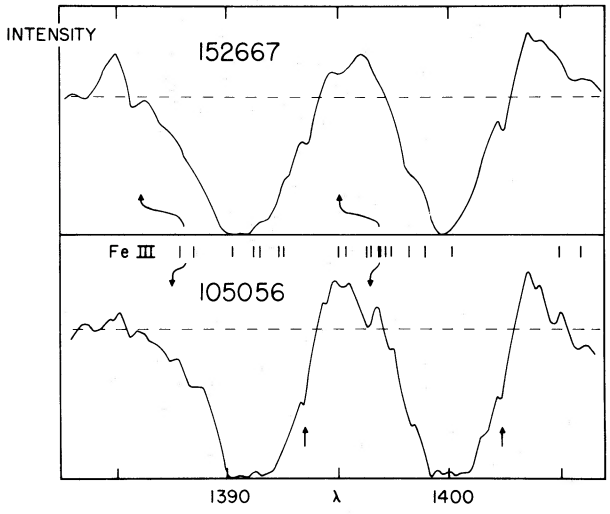

FIG. 4.—Mean of all Si IV profiles for HD 152667, and of two profiles of similar star HD 105056. Grid of weak Fe III lines fits best to two spectra at differing blue shifts (-450, -130 km s^{-1}) as shown. Interstellar absorption components of Si IV indicated by arrows.

V. OTHER STRONG LINE FEATURES

a) The Mg II *Lines*

The profiles of the Mg II $\lambda 2800$ resonance lines are shown in Figure 5. These profiles show a strong component at zero velocity, shifted components at -450 km s^{-1}, and a variable intensity absorption which appears near -100 km s^{-1} in phases ~ 0.5 to 1.0. The -450 km s^{-1} components are broad and variable but show no clear phase-related profile changes. However the shifted line *velocities* bear some resemblance to the orbital velocity range (Fig. 6).

Weak lines in this region of the spectrum were measured for velocity by an overlay best fit. They are found to be close to zero (3 ± 7 km s^{-1}) and not varying significantly. The Mg II line cores have velocity 7 ± 1 km s^{-1}.

The presence of two Mg II absorption systems with different velocities is of interest. The behavior of the low-velocity absorption is suggestive of the wake behavior seen in HD 77581 at Hβ by Zuiderwijk (1979). The low velocity and range of the variation

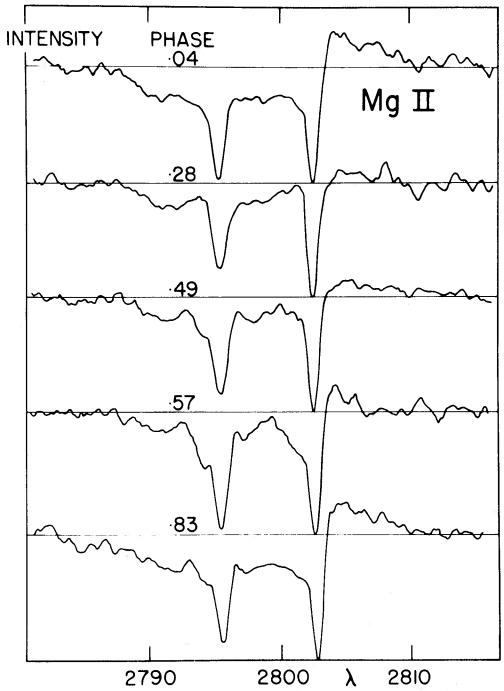

FIG. 5.—Mg II $\lambda 2800$ resonance-line profiles; strong absorptions are largely interstellar. Note variable velocity shifted absorptions, probably formed in stream spiraling out from system.

indicates that it must be formed at a deep level in the wind and probably reflects some of the orbital motion of the primary stars.

b) *The* Al III *lines*

The Al III resonance lines at $\sim\lambda 1850$ also show multiple absorption structure: a sharp interstellar feature, a deep absorption at $\sim -650\ \mathrm{km\ s^{-1}}$, and other variable features at intermediate velocities. Here again, the lower velocity absorption appears to move with the primary star, with a mean velocity of some $-430\ \mathrm{km\ s^{-1}}$. Other weak lines in the region show orbital velocity changes, although again there appear to be significant deviations from the motion of the underlying star (Fig. 6).

The absorption equivalent widths of Al III show changes of less than 10%, which are probably not significant. A weak emission component exists in both lines.

c) Si III *Nonresonance lines*

The region near $\lambda 1300$ contains a number of strong Si III lines and interstellar lines principally of Si II, C II, and O I (Fig. 7). Again, the situation is complex. The C II interstellar lines at $\lambda 1335$ also have shifted components which are quite narrow but variable. The shift is about $-575\ \mathrm{km\ s^{-1}}$. The Si III line also shows a shift of this magnitude. However, a weaker unshifted multiplet is also seen, which takes part in orbital motion with V_0 about $-70\ \mathrm{km\ s^{-1}}$ (Fig. 6). More absorption lines are seen in phases 0.5 to 1.0, and the shifted C II lines are broader in these phases. The shifted system is weaker at $\phi_x \sim 0.5$.

VI. GENERAL REMARKS

The spectrum of HD 152667 in the UV presents a complex picture of mass motions. The terminal wind velocity is within the normal range for the stellar type and luminosity. However, many lines or line components also show relatively sharp absorptions at velocities in the -400 to $-600\ \mathrm{km\ s^{-1}}$ range, as well as "photospheric" components (Table 2). This behavior is unique as far as we know at present and is presumably related to the presence of a massive companion. There is occasionally evidence of (1) a "hole" in the wind at high velocities associated with

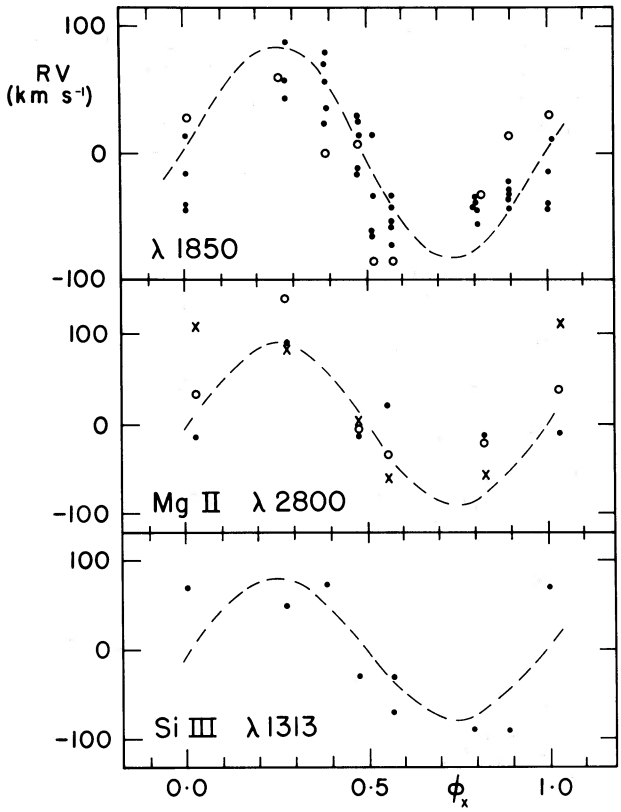

FIG. 6.—Radial velocity measures of HD 152667 from *IUE* data. *Upper.*—*circles*, Al III weak components; *dots*, other individual weak line features in $\lambda 1800$ region. All broken curves are photospheric orbital motion from visual spectrum data. *Center.*—X, Mg II $\lambda 2803$; O, Mg II $\lambda 2795$; *dots*, mean of weaker low velocity components: zero points adjusted to give mean velocity zero. *Lower.*—mean of weak components of Si III line near $\lambda 1300$.

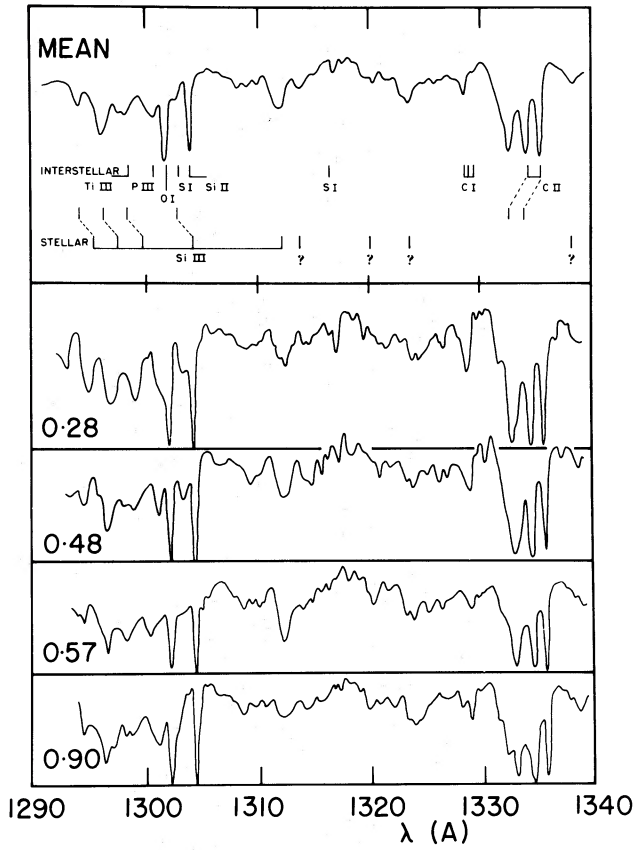

FIG. 7.—Tracings of $\lambda 1300$ region in HD 152667, smoothed over 0.15 Å. *Upper.*—mean spectrum with principal stellar and interstellar absorptions identified. Note presence of shifted and unshifted components of Si III and C II lines. *Lower.*—tracings show changes and corresponding orbital phases.

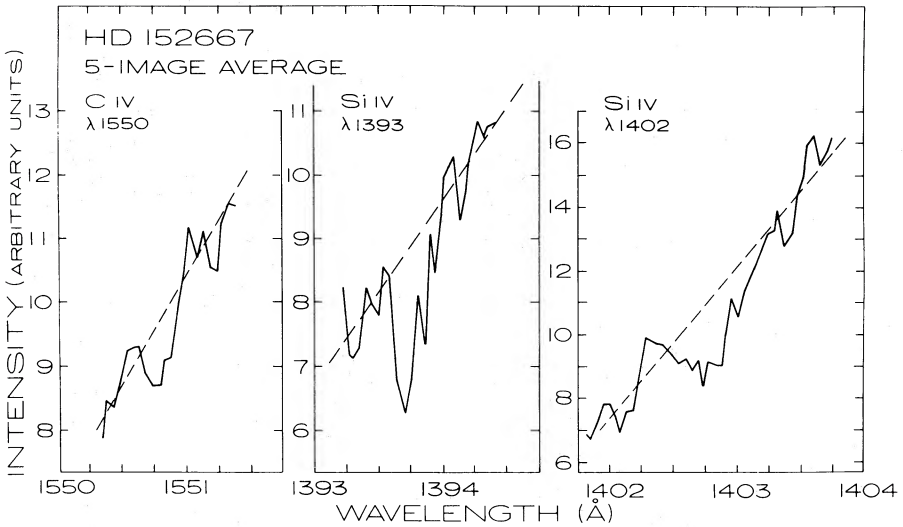

FIG. 8.—Interstellar absorption lines of highly ionized species C IV and Si IV in averaged spectra of HD 152667. The broken line indicates the assumed continuum.

the secondary and (2) enhanced absorption in phases 0.5–1.0. This latter phenomenon is also seen in ground-based data. It may be relevant to note that York *et al.* (1977) found variations in the resonance line profiles of two OB stars at velocities less than 0.5 of the terminal velocity.

The sharp absorptions at velocities -400 to -600 km s^{-1} may arise in a region of enhanced density in a spiraling gas stream surrounding the system. Such a stream would arise if the mass transfer rate exceeds the secondary accretion rate by a large factor.

The UV spectra thus gives no real confirmation of the presence of X-rays from the secondary, but we do see considerable evidence for a complex wind structure which may be related to the presence of the companion.

VII. INTERSTELLAR LINES

As expected for a highly reddened star, many interstellar absorption lines are prominent in the high-dispersion spectrum. The highly ionized species are of particular interest since they may arise in the H II region surrounding the star and can be strengthened if X-rays are produced by the system (McCray, Wright, and Hatchett 1977).

Five high-dispersion images (SWP 1993, 2010, 2101, 2366, 2916) were averaged together by aligning individual orders either at the starting resolution element per order or by alignment on a strong interstellar line in the order itself. The resultant equivalent widths changed by less than a few percent between the two methods. A least-squares polynomial technique was used to fit the continuum on either side of the line; the formal errors in the equivalent-width measurement result from the uncertainty in the fit to the continuum. Both components of the doublets in C IV and N V could not be measured because of the presence of broad absorption components in the stellar P Cygni profiles and the resultant lack of an ultraviolet continuum. Profiles of the highly ionized species of C IV and Si IV are shown in Figure 8. Equivalent widths are given in

TABLE 3

INTERSTELLAR LINES OF HIGHLY IONIZED SPECIES

Ion	λ_{vacuum} (Å)	W (Å)[a] HD 152667	log N (cm^{-2}) HD 152667	log N (cm^{-2})[b] HD 77581	log N (cm^{-2})[c] HD 153919
C IV	1548.185	No signal	...	...	...
	1550.774	0.018C	12.97	14.72	13.71
Si IV	1393.755	0.062B	12.98	13.73	≥13.36
	1402.770	0.075B	13.41		
N V	1238.821	<0.018C	<12.9	...	...
	1242.804	<0.016C	<13.2	...	<13.74

[a] Uncertainties in the equivalent width: B (10–20%); C (>20%).
[b] From Dupree *et al.* 1980.
[c] From Dupree *et al.* 1978.

Table 3. Assuming that the interstellar lines are broadened with $b = 10$ km s^{-1} as found from line-profile calculations for several stars (Black *et al.* 1980), and adopting the oscillator strengths given by Morton and Smith (1973), we obtain the column densities in Table 3. Included also are results for two other reddened binaries (which are X-ray sources): HD 77581 (Vela X-1), another B0 I supergiant, with $E(B-V) = 0.7$; and HD 153919, an O6f star with $E(B-V) = 0.52$ that is near to HD 152667, identified with the X-ray source 4U 1700−37.

The highly ionized species are clearly not of the strength found toward the known X-ray sources, but are more comparable with the values for normal high-luminosity stars (Black *et al.* 1980). The ratios of C IV/Si IV column densities are consistent with those of a photoionized volume. Calculations by Black *et al.* (1979) show that a normal B0 supergiant will produce amounts of C IV and Si IV comparable with the column densities found here.

Of particular interest is the N V transition, for it is difficult to produce this species in an H II region surrounding a B0 supergiant. The upper limits given in the table must be treated with caution since the exposure level is very low in this region. A long exposure to determine its presence would be useful. It may be that the line of sight to HD 152667 intersects the photoionized volume of HD 153919, a strong X-ray source only ~3° away, corresponding to ~60 pc at a distance of 1.2 kpc. Further mapping of the interstellar material in this region would be of interest.

Thus the interstellar spectrum of highly ionized species reflects the abundance of C IV and Si IV that might be expected in the H II region surrounding a normal B0 supergiant, and no evidence is found for excessive ionization produced by a source of X-rays.

IX. CONCLUSION

The UV spectra of the system HD 152667 have revealed the presence of a complex stellar wind, with variable shifted absorptions in the velocity range −400 to −600 km s^{-1}, well below the terminal velocity of ~1400 km s^{-1}. These absorptions are thought to arise in an outwardly spiraling gas stream within the wind, which is probably initiated as a flow from the inner Lagrangian point of the tidally distorted primary. Similar phenomena have been seen in the X-ray binary HD 153919. The UV light curve is principally attributable (as is the visible light curve) to the tidal distortion of the primary, but there is extra light from the secondary at all wavelengths. No line features attributable to the secondary are seen. In order to understand the system better, a new visible region photometric investigation is needed, and a high-sensitivity pointing with the *Einstein* Observatory.

We are very grateful to the *IUE* Observatory staff for their part in obtaining these data, to G. Hill for some of the observations, and to R. Polidan, S. Rowntree, J. Black, and J. Raymond for help and discussion. Partial support for this analysis was provided by NASA grant NSG 5370 to the Harvard College Observatory.

REFERENCES

Black, J. H., Dupree, A. K., Hartmann, L., and Raymond, J. C. 1980, *Ap. J.*, submitted.
Bohlin, R. C., and Snijders, M. A. J. 1978, *IUE Calibration Memo* VI.
Cousins, A. W. J., and Lagerwey, H. C. 1969, *M.N.A.S.So.Africa*, **28**, 120.
Dupree, A. K. *et al.* 1978, *Nature*, **275**, 400.
———. 1980, *Ap. J.*, in press.
Fahlman, G., and Walker, G. A. H. 1979, preprint.
Flower, P. J. 1977, *Astr. Ap.*, **54**, 31.
Hack, M., Hutchings, J. B., Kondo, Y., and McCluskey, G. 1977, *Ap. J. Suppl.*, **34**, 565.
Hill, G., Crawford, D. L., and Barnes, J. V. 1974, *Pub.A.S.P.*, **86**, 477.
Holt, S. S. 1979, private communication.
Hutchings, J. B. 1979*a*, *M.N.R.A.S.*, **187**, 53P.
Hutchings, J. B. 1979*b*, *Ap. J.*, **233**, 913.
Hutchings, J. B., and von Rudloff, I. R. 1980, *Ap. J.*, in press.
Kurucz, R. 1979, *Ap. J. Suppl.*, **40**, 1.
Massey, P., Conti, P. S., Peters, G. J., Dobias, J. 1979, *Ap. J.*, **231**, 171.
McCray, R., Wright, C. and Hatchett, S. 1977, *Ap. J.* (*Letters*), **211**, L29.
Morton, D. G., and Smith, W. H. 1973, *Ap. J. Suppl.*, **26**, 333.
Polidan, R. S., Pollard, G. S. G., Sanford, P. W., and Locke, M. C. 1978, *Nature*, **275**, 296.
Polidan, R. S., Oegerle, W. R., Pollard, G. S. G., Sanford, P. W., and Parmar, A. N. 1979, *Ap. J.* (*Letters*), **233**, L7.
Thompson, G. I. *et al.* 1978, *Catalogue of Stellar UV Fluxes* (Ottawa: SRC).
Walker, E. N. 1971, *M.N.R.A.S.*, **152**, 333.
White, N. E., and Pravdo, S. H. 1979, *Ap. J.* (*Letters*), **233**, L121.
Wolff, S. C., and Beichmann, C. A. 1979, *Ap. J.*, **230**, 519.
York, D. C., Vidal-Madjar, A., Laurent, C., and Bonnet, R. 1977, *Ap. J.* (*Letters*), **213**, L61.
Zuiderwijk, E. J. 1979, thesis, University of Amsterdam.

A. K. DUPREE: Center for Astrophysics, Harvard College Observatory, 60 Garden Street, Cambridge, MA 02138
J. B. HUTCHINGS: Dominion Astrophysical Observatory, 5071 W. Saanich Road, Victoria, B.C., V8X 3X3, Canada